Electrochemical Resistive-Pulse Sensing

Rongrong Pan,[†,§] Keke Hu,[†] Dechen Jiang,[§,*] Uri Samuni,[†] and Michael V. Mirkin[†,*]

[†] Department of Chemistry and Biochemistry, Queens College-CUNY, Flushing, NY 11367, USA.

§ State Key Laboratory of Analytical Chemistry for Life and School of Chemistry and Chemical Engineering, Nanjing University, Nanjing 210023, P. R. China

Supporting Information Placeholder

ABSTRACT: Resistive-pulse sensing with biological or solid-state nanopores and nanopipettes has been widely employed in detecting single molecules and nanoparticles. The analytical signal in such experiments is the change in ionic current caused by the molecule/particle translocation through the pipette orifice. This paper describes a new version of the resistive-pulse technique based on the use of carbon nanopipettes (CNP). The measured current is produced by electrochemical oxidation/reduction of redox molecules at the carbon surface and responds to the particle translocation. In addition to counting single entities, this technique enables qualitative and quantitative analysis of the electroactive material they contain. Using liposomes as a model system, we demonstrate the capacity of CNPs for (1) conventional resistive-pulse sensing of single liposomes, (2) electrochemical resistive-pulse sensing, and (3) electrochemical identification and quantitation of redox species (e.g., ferrocyanide, dopamine and nitrite) contained in a single liposome. The small physical size of a CNP suggests the possibility of single-entity measurements in biological systems.

Resistive-pulse sensing relies on measurements of the ion current flowing through a biological or solid-state nanopore or a nanopipette.[1-5] A nanoparticle (NP),[6] a vesicle,[7-9] or a large molecule[10] entering the nanopore orifice affects its conductance, causing a transient decrease in the ion current (resistive pulse). Nanopore-based techniques have been widely used to sequence DNA,[11] detect singe molecules,[12,13] NPs,[6,14] viruses[15] and nanoparticle-bound species.[16,17] Although nanopore-based sensors are powerful tools for detecting and counting single entities, their applications to qualitative and quantitative analysis are more challenging. Coating the inner wall of the nanocapillary with a thin layer of conductive material, such as Au,[18,19] Pt,[20] carbon,[21,22] Ag,[23] or conductive polymer,[24] yields a nanopore with the tunable surface charge and potential that may improve its selectivity and sensitivity.[25] Conductive nanopores and pipettes have been used for DNA sequencing[26] and detection of small molecules[23] and proteins.[27,28]

We previously produced carbon nanopipettes (CNP) with different geometries by chemical vapor deposition of carbon into quartz capillaries and demonstrated their usefulness for voltammetric sensing.[29,30] Here we employ CNPs (Fig. S1) as a platform for electrochemical resistive-pulse sensing to detect single liposomes and analyze their contents. The performed experiments are shown schematically in Fig. 1. The first one (Fig. 1A) is aimed at checking that liposomes can be detected in a conventional resistive-pulse setup though ion current blockages caused by their translocations of a quartz nanopipette. The current-time recording obtained in such an experiment is shown in Fig. S2A. The current blockages in Fig. S2A were observed with a negative voltage, V = -0.5 V applied to the reference electrode inside the pipette with respect to the external reference. No resistive pulses were recorded with a positive voltage, V = 0.5 V, applied to the pipette (Fig. S2D). This indicates that the translocation of negatively charged liposomes is driven by electroosmosis rather than simple diffusion through the pipette narrow shaft or electrophoresis since the direction of the electroosmotic flow in Fig. S2A was opposite to that of the electrophoresis. In a conceptually similar experiment (Fig. 1B), a CNP was employed for resistive-pulse sensing of liposomes (Fig. S3). The inner surface of a CNP is negatively charged,[31] and the translocation of liposomes is apparently driven by electroosmosis, similar to quartz pipettes.

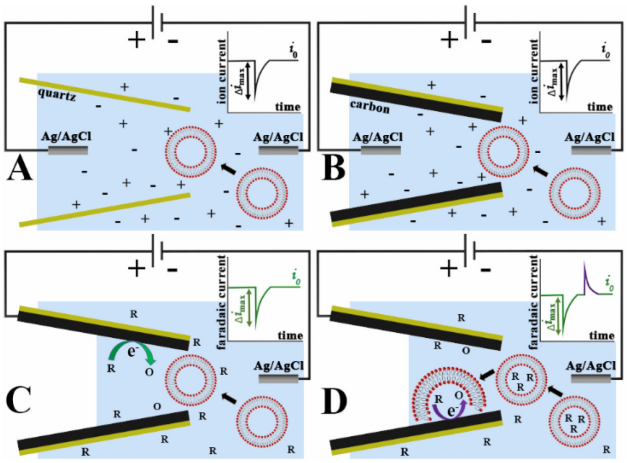

Figure 1. Schematic representation of four types of resistive-pulse experiments involving translocation of liposomes through quartz (A) and carbon (B-D) nanopipettes. The insets show ion current blockages in conventional resistive-pulse sensing (A,B) and faradaic current spikes produced by either a blockage of the CNP orifice (green peaks in C and D) or oxidation/reduction of the redox species contained inside a liposome (purple peak in D). In all experiments, liposomes are initially present only in the outer solution.

Electrochemical resistive-pulse sensing of liposomes is outlined schematically in Fig. 1C. Unlike conventional resistive-pulse experiments, only a small (μm-long) portion of the CNP shaft adjacent to its orifice is filled with solution by capillary force.[22,29] No reference electrode is placed inside the CNP, which serves as a working electrode. The base current (i_0) in this case is produced by diffusion of the redox species to the pipette orifice and their oxidation/reduction at the carbon surface. The blockage of this

current during the liposome (or other particle with a diameter comparable to that of the CNP orifice) translocation results in a resistive pulse (green peak in the inset; Fig. 1C). Because the conductive carbon surface is essentially equipotential, the voltage drop along the pipette axis inside its shaft is small and the translocation of liposomes is driven by diffusion rather than electroosmosis or electrophoresis. Accordingly, the translocation events can be observed at either positive or negative CNP bias with respect to the external reference. The current-time recordings were obtained in solution containing 10 mM of either $K_4[Fe(CN)_6]$ (Fig. 2A) or $K_3[Fe(CN)_6]$ (Fig. 2C), and current blockages by liposomes can be seen at both positive (+0.5 V; Fig. 2A) and negative (-0.5 V; Fig. 2C) CNP potentials.

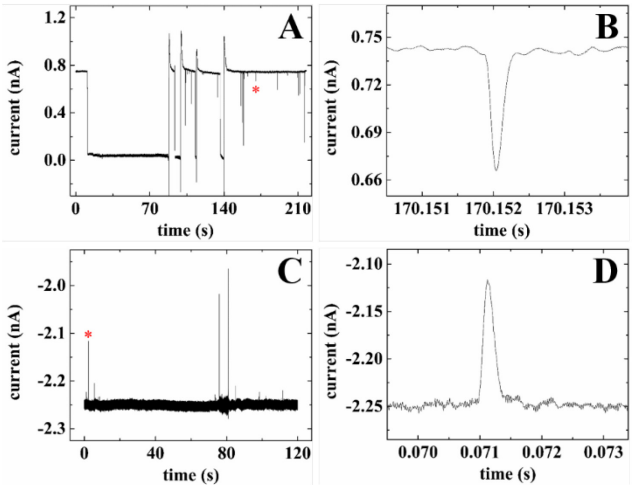

Figure 2. Electrochemical resistive-pulse sensing of liposomes by CNPs in 10 mM PBS (pH 7.4) solution containing 10 mM $K_4[Fe(CN)_6]$ (A) or 10 mM $K_3[Fe(CN)_6]$ (C). CNP potential vs. Ag/AgCl was (A) 0.5 V and (C) -0.5 V. CNP orifice diameter, nm was (A) 270 and (C) 250. Blowups of transients labeled by red asterisks in (A) and (C) are shown in (B) and (D), respectively. Solution contained 15.6 nM of liposomes.

Fig. 2A exhibits markedly different short (sub-ms to ms) and long (hundreds of ms to tens of seconds) spikes. Typical short pulses (Figs. 2B and 2D) have a relatively small magnitude, $\Delta i_{max}/i_0 << 1$, shape, and mean τ values (0.21 and 0.29 ms for $K_4[Fe(CN)_6]$ and $K_3[Fe(CN)_6]$, respectively) similar to those of conventional resistive pulses (Figs. S2C and S3C). By contrast, long resistive pulses in Fig. 2A feature nearly complete current blockages. (Long resistive pulses were also recorded with ferricyanide; not shown). At the end of each long blockage, the current increased sharply to a value higher than i_0. Long translocation events have only been observed in electrochemical resistive-pulse experiments. With no electroosmotic flow inside the CNP shaft, a larger liposome whose diameter is similar to that of the pipette orifice can get stuck at the tip, completely blocking the diffusion current of redox molecules. The abrupt departure (or bursting open) of the liposome apparently produces a sharp transient increase in the current above the base level. Both long and short current blockages are produced by liposomes entering the CNP rather just plugging its orifice from the solution side. By contrast, no current spikes were observed using CNPs with the orifice diameter smaller than that of the liposomes (Fig. S4).

The cathodic base current in Fig. 2C is much higher than the anodic current in Fig. 2A measured with the same concentration of redox species in solution (10 mM) and a similar CNP diameter. The difference is due to a significant cathodic current flowing at a CNP is solution containing no added redox species (Fig. S5). This current is produced by oxygen reduction catalyzed by impurities in the CVD-deposited carbon film. The high rate of oxygen reduction is due to the large surface area of porous carbon film exposed to the aqueous solution. The possibility of electrochemical resistive-pulse sensing with no redox mediator added to solution is shown in Figs. S5A and S5B. By contrast, no significant anodic current flows when a CNP is biased at a positive potential without redox species added to the solution, and no resistive pulses appear in Fig. S5C. The transport of O_2 to the carbon surface includes both the diffusion flux to the CNP orifice and the influx from the air contained inside the CNP capillary (see Fig. S6 and related discussion in SI).

To combine electrochemical resistive-pulse sensing with electroanalysis of single vesicle contents (Fig. 1D), liposomes were loaded with redox species (e.g., $K_4[Fe(CN)_6]$). The presence of $Fe(CN)_6^{4-}$ inside liposomes was confirmed by electrochemical monitoring of their collisions with a carbon ultramicroelectrode that produced ms-long spikes of anodic current (Fig. S7).[32] Resistive-pulse recordings in this case are expected to include current blockages associated with liposome translocations (green peak in Fig. 1D) and current upsurges caused by oxidation/reduction of redox species during liposome collisions with the CNP inner wall (purple peak). Both upward and downward spikes can be seen in current-time recordings obtained with ferrocyanide-loaded liposomes translocating a CNP (Fig. 3A). These current transients cannot be attributed to either blockages of the CNP orifice from the solution side or collisions of liposomes with the carbon ring exposed to the external solution because the recordings obtained with smaller pipettes show no current spikes (Fig. S4E).

The integration of the current yields the charge corresponding to the number $Fe(CN)_6^{4-}$ ions oxidized during a specific collision. The relationship between the charge value (Q) and the liposome radius (r) is given by Eq. (1) [32]

$$Q = \frac{4}{3}\pi r^3 cnF \quad (1)$$

where c is the concentration of $K_4[Fe(CN)_6]$ in the liposome (0.5 M), n = 1 is the number of transferred electrons, and F is the Faraday constant. The distribution of liposome diameters calculated from the charge values is shown in Fig. 3D along with the size distribution from DLS data (black line). The liposome diameters evaluated from resistive-pulse data are somewhat smaller than those found by DLS because the latter technique is skewed toward large size particles, and the measured hydrodynamic radius includes the thickness of the hydration layer of the lipid headgroups.[33,34] By contrast, resistive-pulse measurements may not fully account for larger particles, which are less likely to translocate through a comparably sized pipette orifice.[35] Also, some liposomes may release only a fraction of their redox load during a collision with the carbon surface. (Partial release of neurotransmitters from vesicles was also observed during exocytosis.[36]) The average frequency of upward spikes in Fig. 3A that is higher than the frequency of resistive pulses may be due to multiple collisions of a liposome with the CNP wall. Alternatively, low-amplitude resistive-pulses produced by small liposomes may have been obfuscated by noise and not detected.

Electrochemical resistive-pulse sensing is potentially useful for detection and analysis of biological vesicles such as dopamine (DA) containing synaptic vesicles.[36,37] Fig. 4A shows a current-time recoding obtained with DA-loaded liposomes translocating a 350-nm-diameter CNP. Similar to the data in Fig. 3, this recoding comprises resistive pulses and upward spikes produced by oxidation of dopamine during liposome collisions with the CNP wall. Typical resistive pulse and collision transients are shown in Figs. 4B and 4C, respectively. The widths and shapes of these spikes are

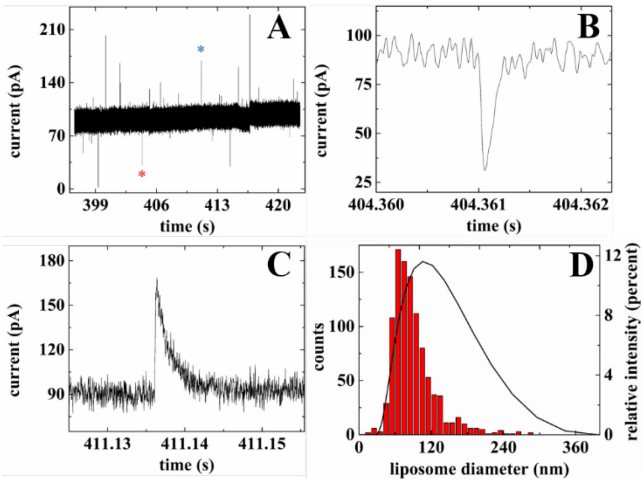

Figure 3. Electrochemical resistive-pulse sensing of ferrocyanide-loaded liposomes and electrochemical analysis of their contents. (A) Current-time recording obtained with a 495-nm CNP biased at +0.5 V vs. Ag/AgCl reference. (B) Individual resistive-pulse spike labeled with a red asterisk in A. (C) Representative liposome collision transient labeled with a blue asterisk in A. (D) Distribution of liposome diameters calculated from the charge values (bar graph; the left-hand scale) and liposome size distribution from DLS data (black line; the right-hand scale).

comparable to those obtained with ferrocyanide-loaded liposomes (Figs 3B and 3C). The cyclic voltammogram in Fig. 4D obtained with the same pipette immediately after an electrochemical resistive-pulse experiment, comprises a pair of symmetrical peaks of exhaustive oxidation/reduction of DA accumulated inside the CNP. The midpoint potential, 0.1 V vs. Ag/AgCl, is in good agreement with reported CNP voltammograms of DA.[30]

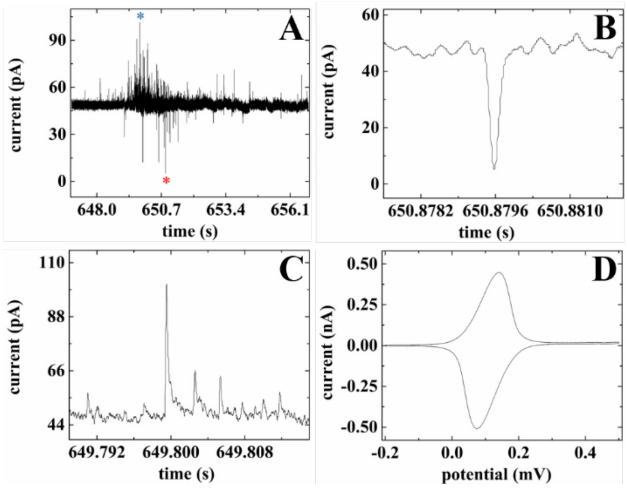

Figure 4. Electrochemical resistive-pulse sensing of dopamine-loaded single liposomes. (A) Current-time recording obtained with DA-loaded liposomes using a 350 nm CNP. (B) Individual resistive pulse labeled with a red asterisk in A. (C) Representative liposome collision transient labeled with a blue asterisk in A. CNP potential was 0.5 V vs. Ag/AgCl. (D) Cyclic voltammogram of DA. Potential sweep rate, v = 50 mV/s.

Another type of physiologically important species stored in biological vesicles are reactive oxygen and nitrogen species (ROS/RNS). Platinized micro- and nanoelectrodes have previously been used for measuring ROS/RNS in biological systems,[38] including single vesicle analysis.[39,40] To explore the possibility of electrochemical resistive-pulse sensing of ROS/RNS in single vesicles, we prepared platinized CNPs (Fig. S8A) and loaded liposomes with nitrite solution. Nitrite—one of four primary ROS/RNS—tends to strongly passivate electrode surfaces and is, therefore, hard to measure.[38] Resistive-pulse recordings and oxidation current transients of NO_2^--loaded liposomes obtained with platinized CNPs are shown in Figs. S8B and S8C. A cyclic voltammogram obtained after the electrochemical resistive-pulse experiment (Fig. S8D) can be used to identify nitrite species.

In conclusion, we used CNPs as a platform for electrochemical resistive-pulse sensing. In this new technique, faradaic current produced by oxidation/reduction of redox species at the carbon surface (as opposed to ion current measured in conventional resistive-pulse experiments) is used to detect nanoscopic objects, such as liposomes, translocating through the CNP orifice. In addition to counting single entities, this approach enables electrochemical analysis of the contents of liposomes (or other nanovesicles) by measuring current transients produced by their collisions with the inner wall of the CNP. In this way, dopamine and nitrite were measured in single liposomes. In a recent study,[41] we demonstrated the possibility of conventional resistive-pulse sensing of biological vesicles inside a living cell and near its surface. Electrochemical resistive-pulse sensing developed here can enable sampling and determination of important biochemical species (e.g., neurotransmitters and ROS/RNS) stored in such vesicles.[36,39]

ASSOCIATED CONTENT

Supporting Information. Experimental details, additional resistive-pulse recordings and voltammograms, and TEM images of CNPs, including Figures S1 – S8 and Table S1. This material is available free of charge via the Internet at http://pubs.acs.org.

AUTHOR INFORMATION

Corresponding Authors
* mmirkin@qc.cuny.edu; dechenjiang@nju.edu.cn

Notes
The authors declare no competing financial interests.

ACKNOWLEDGMENT

The support of this work by the National Science Foundation (CHE-1763337) is gratefully acknowledged.

REFERENCES

(1) Bayley, H.; Martin, C. R. Resistive-Pulse Sensing-From Microbes to Molecules. *Chem Rev* **2000**, *100*, 2575-2594.
(2) Venkatesan, B. M.; Bashir, R. Nanopore Sensors for Nucleic Acid Analysis. *Nat. Nanotechnol.* **2011**, *6*, 615-624.
(3) Stoloff, D. H.; Wanunu, M. Recent trends in nanopores for biotechnology. *Curr. Opin. Biotech.* **2013,** *24*, 699-704.
(4) Shi, W.; Friedman, A. K.; Baker, L. A. Nanopore Sensing. *Anal. Chem.* **2017**, *89*, 157-188.
(5) Wang, Y.; Wang, D.; Mirkin, M. V. Resistive-pulse and Rectification Sensing with Glass and Carbon Nanopipettes. *Proc. R. Soc. London Ser. A* **2017**, *473*, 20160931.
(6) Luo, L.; German, S. R.; Lan, W.-J.; Holden, D. A.; Mega, T. L.; White, H. S. Resistive-pulse Analysis of Nanoparticles. *Annu. Rev. Anal. Chem.* **2014**, *7*, 513-535.
(7) Rudzevich, Y.; Lin, Y.; Wearne, A.; Ordonez, A.; Lupan, O.; Chow, L. Characterization of Liposomes and Silica Nanoparticles using Resistive Pulse Method. *Colloid Surf. A-Physicochem. Eng. Asp.* **2014**, *448*, 9-15.
(8) Chen, L.; He, H.; Jin, Y. Counting and Dynamic Studies of the Small Unilamellar Phospholipid Vesicle Translocation with Single Conical Glass Nanopores. *Anal. Chem.* **2015**, *87*, 522-529.
(9) Liu, Y.; Xu, C.; Chen, X.; Wang, J.; Yu, P.; Mao, L. Voltage-driven Counting of Phospholipid Vesicles with Nanopipettes by Resistive-pulse Principle. *Electrochem. Commun.* **2018**, *89*, 38-42.
(10) Howorka, S.; Siwy, Z. Nanopore Analytics: Sensing of Single Molecules. *Chem. Soc. Rev.* **2009**, *38*, 2360–2384.
(11) Branton, D.; Deamer, D. W.; Marziali, A.; Bayley, H.; Benner, S. A.; Butler, T.; Di Ventra, M.; Garaj, S.; Hibbs, A.; Huang, X. H.; Jovanovich, S. B.;

Krstic, P. S.; Lindsay, S.; Ling, X. S. S.; Mastrangelo, C. H.; Meller, A.; Oliver, J. S.; Pershin, Y. V.; Ramsey, J. M.; Riehn, R.; Soni, G. V.; Tabard-Cossa, V.; Wanunu, M.; Wiggin, M.; Schloss, J. A. The Potential andChallenges of Nanopore Sequencing. *Nat. Biotechnol.* **2008,** *26*, 1146-1153.

(12) Heins, E. A.; Siwy, Z. S.; Baker, L. A.; Martin, C. R. Detecting Single Porphyrin Molecules in a Conically Shaped Synthetic Nanopore. *Nano Lett.* **2005**, *5*, 1824-1829.

(13) Miles, B. N.; Ivanov, A. P.; Wilson, K. A.; Dogan, F.; Japrung, D.; Edel, J. B. Single molecule sensing with solid-state nanopores: novel materials, methods, and applications. *Chem Soc Rev* **2013,** *42*, 15-28.

(14) Tsutsui, M.; Hongo, S.; He, Y. H.; Taniguchi, M.; Gemma, N.; Kawai, T. Single-nanoparticle Detection using a Low-aspect-ratio Pore. *ACS Nano* **2012,** *6*, 3499-3505.

(15) Terejánszky, P.; Makra, I.; Fürjes, P.; Gyurcsányi, R. E. Calibration-less Sizing and Quantitation of Polymeric Nanoparticles and Viruses with Quartz Nanopipets. *Anal. Chem.* **2014**, *86*, 4688–4697.

(16) Wang, Y. X.; Kececi, K.; Mirkin, M. V.; Mani, V.; Sardesai, N.; Rusling, J. F. Resistive-pulse Measurements with Nanopipettes: Detection of Au Nanoparticles and Nanoparticle-bound Anti-peanut IgY. *Chem. Sci.* **2013,** *4*, 655-663.

(17) Lin, X.; Ivanov, A. P.; Edel, J. B. Selective single molecule nanopore sensing of proteins using DNA aptamer-functionalised gold nanoparticles. *Chem. Sci.* **2017**, *8*, 3905–3912.

(18) Freedman, K. J.; Otto, L. M.; Ivanov, A. P.; Barik, A.; Oh, S. H.; Edel, J. B. Nanopore sensing at ultra-low concentrations using single-molecule dielectrophoretic trapping. *Nat. Commun.* **2016,** *7*. 10217.

(19) Yang, C.; Hinkle, P.; Menestrina, J.; Vlassiouk, I. V.; Siwy, Z. S. Polarization of Gold in Nanopores Leads to Ion Current Rectification. *J. Phys. Chem. Lett.* **2016,** *7*, 4152-4158.

(20) Pan, R.; Xu, M.; Burgess, J. D.; Jiang, D.; Chen, H.-Y. Direct electrochemical observation of glucosidase activity in isolated single lysosomes from a living cell. *Proc. Natl. Acad. Sci. U.S.A.* **2018,** *115*, 4087-4092.

(21) Singhal, R.; Bhattacharyya, S.; Orynbayeva, Z.; Vitol, E.; Friedman, G.; Gogotsi, Y. Small diameter carbon nanopipettes. *Nanotechnology* **2010,** *21*. 241.

(22) Hu, K. K.; Wang, Y. X.; Cai, H. J.; Mirkin, M. V.; Gao, Y.; Friedman, G.; Gogotsi, Y. Open Carbon Nanopipettes as Resistive-Pulse Sensors, Rectification Sensors and Electrochemical Nanoprobes. *Anal. Chem.* **2014,** *86*, 8897-8901.

(23) Gao, R.; Ying, Y.-L.; Hu, Y.-X.; Li, Y.-J.; Long, Y.-T. Wireless Bipolar Nanopore Electrode for Single Small Molecule Detection. *Anal. Chem.* **2017**, *89*, 7382−7387.

(24) Perez-Mitta, G.; Marmisolle, W. A.; Trautmann, C.; Toimil-Molares, M. E.; Azzaroni, O. Nanofluidic Diodes with Dynamic Rectification Properties Stemming from Reversible Electrochemical Conversions in Conducting Polymers. *J. Am. Chem. Soc.* **2015,** *137*, 15382-15385.

(25) Yu, R.-J.; Ying, Y.-L.; Gao, R.; Long, Y.-T. Confined Nanopipette Sensing: From Single Molecules, Single Nanoparticles, to Single Cells. *Angew. Chem., Int. Ed.* **2019**, *58*, 3706-3714.

(26) Banerjee, S.; Shim, J.; Rivera, J.; Jin, X. Z.; Estrada, D.; Solovyeva, V.; You, X.; Pak, J.; Pop, E.; Aluru, N.; Bashir, R. Electrochemistry at the Edge of a Single Graphene Layer in a Nanopore. *ACS Nano* **2013,** *7*, 834-843.

(27) Siwy, Z.; Trofin, L.; Kohli, P.; Baker, L. A.; Trautmann, C.; Martin, C. R. Protein Biosensors Based on Functionalized Conical Gold Nanotubes. *J. Am. Chem. Soc.* **2005**, *127*, 5000−5001.

(28) Rutkowska, A.; Freedman, K.; Skalkowska, J.; Kim, M. J.; Edel, J. B.; Albrecht, T. Electrodeposition and bipolar effects in metallized nanopores and their use in the detection of insulin. *Anal. Chem.* **2015,** *87*, 2337-2344.

(29) Bae, J. H.; Wang, D.; Hu, K.; Mirkin, M. V. Surface Charge Effects on Voltammetry in Carbon Nanocavities. *Anal. Chem.* **2019**, *91*, 5530–5536.

(30) Yang, C.; Hu, K.; Wang, D.; Zubi, Y.; Lee, S. T.; Puthongkham, P.; Mirkin, M. V.; Venton, B. J. Cavity Carbon Nanopipette Electrodes for Dopamine Detection. *Anal. Chem.* **2019**, *91,* 4618−4624.

(31) Wang, D.; Mirkin, M. V. Electron-Transfer Gated Ion Transport in Carbon Nanopipettes. *J. Am. Chem. Soc.* **2017***, 139,* 11654–11657.

(32) Lebègue, E.; Anderson, C. M.; Dick, J. E.; Webb, L. J.; Bard, A. J. Electrochemical Detection of Single Phospholipid Vesicle Collisions at a Pt Ultramicroelectrode. *Langmuir* **2015**, *31*, 11734−11739.

(33) Coldren, B.; van Zanten, R.; Mackel, M. J.; Zasadzinski, J. A. From Vesicle Size Distributions to Bilayer Elasticity via Cryo-Transmission and Freeze-Fracture Electron Microscopy. *Langmuir* **2003,** *19,* 5632-5639.

(34) Zhang, W.; Coughlin, M. L.; Metzger, J. M.; Hackel, B. J.; Bates, F. S.; Lodge, T. P. Influence of Cholesterol and Bilayer Curvature on the Interaction of PPO−PEO Block Copolymers with Liposomes. *Langmuir* **2019**, *35*, 7231−7241.

(35) Cai, H.; Wang, Y.; Yu, Y.; Mirkin, M. V.; Bhakta, S.; Bishop, G. W.; Joshi, A.; Rusling, J. F. Resistive-Pulse Measurements with Nanopipettes: Detection of Vascular Endothelial Growth Factor C (VEGF-C) using Antibody-decorated Nanoparticles. *Anal. Chem.* **2015**, *87*, 6403–6410.

(36) Phan, N. T. N.; Li, X.; Ewing, A. G. Measuring synaptic vesicles using cellular electrochemistry and nanoscale molecular imaging. *Nat. Rev. Chem.* **2017**, *1*, 1-18.

(37) Dunevall, J.; Fathali, H.; Najafinobar, N.; Lovric, J.; Wigström, J.; Cans, A.-S.; Ewing, A. G. Characterizing the Catecholamine Content of Single Mammalian Vesicles by Collision–Adsorption Events at an Electrode. *J. Am. Chem. Soc.* **2015**, *137* (13), 4344-4346.

(38) Amatore, C.; Arbault, S.; Guille, M.; Lemaître, F. Electrochemical monitoring of single cell secretion: vesicular exocytosis and oxidative stress. *Chem. Rev.* **2008**, *108*, 2585-2621.

(39) Li, Y. T.; Zhang, S. H.; Wang, L.; Xiao, R. R.; Liu, W.; Zhang, X. W.; Zhou, Z.; Amatore, C.; Huang, W. H. Nanoelectrode for Amperometric Monitoring of Individual Vesicular Exocytosis inside Single Synapses. *Angew. Chem. Int. Ed.* **2014**, 53, 12456-12460.

(40) Hu, K.; Li, Y.; Rotenberg, S. A.; Amatore, C.; Mirkin, M. V. Electrochemical Measurements of Reactive Oxygen and Nitrogen Species Inside Single Phagolysosomes of Living Macrophages. *J. Am. Chem. Soc.* **2019**, *141*, 4564−4568.

(41) Pan, R.; Hu, K.; Jiang, D.; Rotenberg, S. A.; Mirkin, M. V. Resistive-Pulse Sensing Inside Single Living Cells. *Manuscript in preparation*.

For TOC only